Impacts of meteorological uncertainties on ozone pollution predictability estimated through meteorological and photochemical ensemble forecasts

Fuqing Zhang,[1] Naifang Bei,[1] John W. Nielsen-Gammon,[1] Guohui Li,[1] Renyi Zhang,[1] Amy Stuart,[1,2] and Altug Aksoy[1,3]

Received 21 April 2006; revised 14 July 2006; accepted 16 August 2006; published 22 February 2007.

[1] This study explores the sensitivity of ozone predictions from photochemical grid point simulations to small meteorological initial perturbations that are realistic in structure and evolution. Through both meteorological and photochemical ensemble forecasts with the Penn State/NCAR mesoscale model MM5 and the EPA Community Multiscale Air Quality (CMAQ) Model-3, the 24-hour ensemble mean of meteorological conditions and the ozone concentrations compared fairly well against the observations for a high-ozone event that occurred on 30 August during the Texas Air Quality Study of 2000 (TexAQS2000). Moreover, it was also found that there were dramatic uncertainties in the ozone prediction in Houston and surrounding areas due to initial meteorological uncertainties for this event. The high uncertainties in the ozone prediction in Houston and surrounding areas due to small initial wind and temperature uncertainties clearly demonstrated the importance of accurate representation of meteorological conditions for the Houston ozone prediction and the need for probabilistic evaluation and forecasting for air pollution, especially those supported by regulating agencies.

Citation: Zhang, F., N. Bei, J. W. Nielsen-Gammon, G. Li, R. Zhang, A. Stuart, and A. Aksoy (2007), Impacts of meteorological uncertainties on ozone pollution predictability estimated through meteorological and photochemical ensemble forecasts, *J. Geophys. Res.*, *112*, D04304, doi:10.1029/2006JD007429.

1. Introduction

[2] Uncertainties associated with photochemical grid model simulations of air quality are varied and complex [*Fine et al.*, 2003]. Despite the theoretical and practical need to quantify these uncertainties [*Dabberdt et al.*, 2004], few attempts have been made to investigate meteorological uncertainties and their role in limiting the expected accuracy of deterministic photochemical simulations. The purpose of this study is to investigate the sensitivity of grid model ozone simulations of a major urban area to small initial perturbations of meteorological variables that are realistic in structure and evolution.

[3] Past attempts to investigate photochemical sensitivity to meteorological uncertainty have included Monte Carlo simulations with randomly specified meteorological and photochemical variables [*Hanna et al.*, 2001; *Beekmann and Derognat*, 2003] and adjoint sensitivity studies of meteorological and photochemical variables [*Menut*, 2003]. Such studies do not treat meteorological variability in a comprehensive and dynamically consistent manner. The Monte Carlo simulations attempt to span the range of uncertainties of the input parameters by quasi-random sampling from a specified probability distribution for each parameter. The adjustments to meteorological fields are uniform in space and/or time, ignoring the true nature of meteorological variability and the differences in meteorological uncertainty across scales [*Hogrefe et al.*, 2001]. Adjoint studies determine the linear sensitivity about a control parameter set. These computed sensitivities are valid only in the neighborhood of the control simulation, and in the case of sensitivity to wind, that neighborhood is likely to be quite small [*Yegnan et al.*, 2002].

[4] Lagrangian dispersion models have also been studied with Monte Carlo sensitivity analyses [*Irwin et al.*, 1987; *Stuart et al.*, 1996; *Bergin et al.*, 1999; *Dabberdt and Miller*, 2000]. Unlike photochemical simulations, however, Lagrangian model sensitivity analysis has also utilized variable meteorology arising from different initial conditions or model configurations [*Straume*, 2001; *Warner et al.*, 2002], culminating in the multinational ENSEMBLE project [*Galmarini et al.*, 2004a]. These experiments include realistic meteorological scenarios by design, but in many cases the meteorological variability has been large-scale in nature.

[5] Very recently, the ensemble approaches with Eulerian grid models has recently been applied to photochemical modeling such as through the use of different transport

[1]Department of Atmospheric Sciences, Texas A&M University, College Station, Texas, USA.
[2]Now at Department of Environmental and Occupational Health, University of South Florida, Tampa, Florida, USA.
[3]Now at National Center for Atmospheric Research, Boulder, Colorado, USA.

0148-0227/07/2006JD007429

models and photochemical reactions [*Delle Monache and Stull*, 2003], different long-range transport and dispersion models [*Galmarini et al.*, 2004b, 2004c], different physical parameterizations [*Mallet and Sportisse*, 2006], different air quality forecasts models [*McKeen et al.*, 2005], different meteorological and photochemical models together with different emission scenarios [*Delle Monache et al.*, 2006a]. In all cases, the ensemble means performed better than most models individually. Recent studies also demonstrated that the air quality forecasts can be further improved through weighted ensemble means [e.g., *Delle Monache et al.*, 2006b; *Pagowski et al.*, 2005].

[6] Photochemical simulations of urban air pollution events must accurately reproduce local, mesoscale, and larger-scale meteorological variations and their interactions, particularly when the urban area is located in a mountainous or coastal area. Houston, Texas, for example, is subject to frequent high-ozone episodes, and the meteorological circumstances associated with high ozone typically involve stagnation or recirculation associated with the sea breeze [*Banta et al.*, 2005; *Darby*, 2005]. The sea breeze is perhaps one of the most extensively studied phenomena in atmospheric dynamics [e.g., *Estoque*, 1962; *Rotunno*, 1983; *Simpson*, 1994], and accurate modeling of the sea breeze requires correct reproduction of the broader meteorological conditions as well as the fluxes that drive the sea breeze itself. With respect to initial meteorological conditions, both meteorological and photochemical forecasts of the Houston area have been shown to be extremely sensitive to different initial conditions derived from different operational weather prediction models [*Bao et al.*, 2005].

[7] The 30 August 2000 Houston ozone event is a classic example of the interaction between ozone and local meteorology. Skies were clear and temperatures were close to 40°C at inland locations. Hour-averaged ozone levels approached 200 ppb at several monitors between Houston and Galveston Bay. Both the observational study of *Banta et al.* [2005] and the modeling study of *Bao et al.* [2005] showed that the sea breeze circulation under weak synoptic flow contributed greatly to the occurrence of this extreme ozone event.

[8] The impacts of realistic meteorological uncertainties on ozone pollution predictability will be demonstrated through ensemble forecasts of the 30 August event, using state-of-the-art meteorological and photochemical prediction models. The experimental design will be given in section 2. The control ensemble simulations and sensitivity experiments will be respectively presented in sections 3 and 4. Section 5 will summarize the study.

2. Forecast Models, Ensemble Generation, and Experimental Design

[9] The Pennsylvania State University-National Center for Atmospheric Research (Penn State-NCAR) fifth-generation nonhydrostatic mesoscale model (MM5) version 3 [*Dudhia*, 1993] is used to represent the numerical and implementation complexities associated with an operational forecasting system. The 12-km coarse model domain (D1) covers an area of 1200 km by 1200 km over mostly the south central United States and the northwestern part of Gulf of Mexico. The one-way nested 4-km fine domain (D2) covers an area of 600 km by 540 km centered on the Houston area (Figure 1). There are 43 layers in the terrain-following vertical coordinate with the model top at 50 hPa (approximately 20 km) and vertical spacing smallest within the boundary layer. The MRF boundary layer parameterization scheme of *Hong and Pan* [1996] and the simple ice microphysical scheme of *Dudhia* [1993] are used for both the 12-km and 4-km domain. The cumulus scheme of *Grell* [1993] with the shallow cumulus option is used only for the 12-km domain while the 4-km domain is fully explicit.

[10] All MM5 simulations are performed in an ensemble setting with 21 members initialized at 0000 UTC 30 August 2000 (1800 LST 29 August 2000) and integrated for 24 hours. To reflect the climatological variability of the state of the atmosphere during summer months, a climatological ensemble initialization method is devised in which dynamically consistent initial and boundary conditions are statistically sampled from a seasonal meteorological data set. This scheme is similar to the initialization technique used by *Aksoy et al.* [2005, 2006] for a two-dimensional sea breeze model. To represent the summertime climatological statistics, a data set for the period of 1 June to 15 September 2000 is generated from the Eta model's 3-hourly gridded (40-km) analyses for the Global Energy and Water Cycle Experiment (GEWEX) Continental-Scale International Project (GCIP). Twenty-one ensemble perturbations were randomly selected from this climatological data set. Similarly, boundary conditions for each ensemble member were generated from the GCIP data beginning at the randomly selected initial time of the given member, and extending for the same length of time as the control run.

[11] Deviations of the initial and boundary condition data for each member from the climatological mean for the entire period are then scaled down to 20% to reduce the ensemble spread to below typical observation error magnitudes [see *Kalnay*, 2003, Figure 6.5.6]. Ensemble spread is diagnosed using the standard deviation and referred to simply as "spread" hereafter. The initial spread of u, v, and T at the surface is 0.4–0.6 m s^{-1} and 0.7–0.8 K over the Houston area. The scaled initial and boundary uncertainties are then added to the unperturbed initial and boundary conditions derived directly from the GCIP analyses valid at 0000 UTC 30 August (18 LST 29 August) which are used for the 12-km domain ensemble simulation. This 21-member ensemble simulation ("CNTL") was integrated for 24 hours on both the 12-km and 4-km domains with one-way nesting. The sea surface temperatures and soil moisture of all ensemble members for were derived from the unperturbed GCIP analyses. The MM5 simulations used the 24 land use categories created from the 30-s USGS global land cover data but the land-surface model was not used.

[12] The 12-km and 4-km meteorological ensemble simulations are then used to drive a 21-member photochemical ensemble forecast using the EPA photochemical model CMAQ/Model-3 [*Byun and Ching*, 1999] also with 12-km and 4-km horizontal grid spacings, respectively. The CMAQ model employs 21 vertical layers with the lowest three levels at approximately 21, 64 and 106 m. The CBIV gas-phase chemical mechanism was employed in this study [*EPA*, 2003]. Biogenic emissions are directly downloaded from the online emission inventory of the Texas Commission on Environmental Quality (TCEQ). The same emission

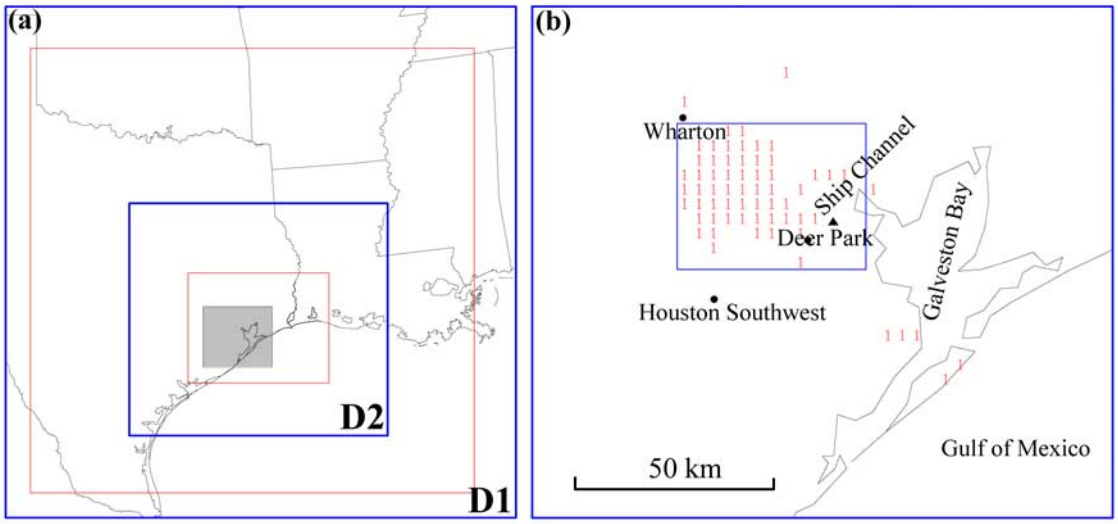

Figure 1. (a) Relative locations of the MM5 (blue boxes) and CMAQ (red boxes) model domains. Grid distances of domain 1 (D1) and domain 2 (D2) are 12 km and 4 km, respectively. (b) Map of the greater Houston region shaded in Figure 1a in which the urbanized area is marked with "1" within urban grid boxes. The inner box in Figure 1b denotes the Houston urban core area.

inventory (including enhanced point source light olefins) and the same chemical model setup are used in all CMAQ ensemble simulations, since here we focus only on the impacts of meteorological uncertainties in the air pollution prediction. Initial conditions for chemistry in the 12-km domain employ the output from a 24-h spin-up simulation (i.e., from 00Z 29 August to 00Z 30 August 2000) by the same CMAQ model running at the same resolution, which were then used to initialize the 4-km fields. The 12-km and 4-km photochemical domains are smaller than the corresponding meteorological simulations (Figure 1a). The emissions inventory was downloaded from the TCEQ anonymous ftp site (ftp.tceq.state.tx.us, emission inventory version base5b.psito2n2) and was then converted to CMAQ-ready emission files. Olefin emissions were increased by a factor of three from all point sources to improve the ozone simulation following *Zhang et al.* [2004]. Such an increase of highly reactive alkenes from petrochemical facilities is justified by several recent studies which concluded that the values of alkenes inferred from measurements made within the downwind plumes were much higher than the emission inventories reported at the TCEQ ftp site [e.g., *Ryerson et al.*, 2003; *Wert et al.*, 2003].

[13] Two sensitivity experiments were also performed. Experiment "half-run" ("double-run") is the same as CNTL for both the meteorological and photochemical ensembles except that the initial (meteorological) ensemble perturbations were reduced by half (doubled). These two experiments are to further examine the role of the meteorological error amplitude in ozone pollution simulation uncertainties.

3. Control Ensemble Simulation

[14] The ensemble mean at the initial time (0000 UTC) features a coastal temperature gradient and a moderate, mostly southerly, sea breeze along the Texas coast that turns southeasterly farther inland (Figures 2a, 2c, 2e, and 3a). For brevity, only results from the 4-km domains of both meteorological and photochemical ensemble simulations will be discussed.

3.1. Overview of the Ensemble Performance

[15] The evolution of the ensemble mean and spread of the surface ozone distributions along with the ensemble mean wind vectors simulated by the CNTL ensemble is shown in Figure 3. At the initial time, the maximum $[O_3]$ of 60–80 ppb is located just north of the Houston area (Figure 3a), and because the chemistry is unperturbed, the initial spread is zero. From 00 to 06 UTC, the maximum ozone concentration moved from the north of the Houston area to the northwest portion of the model inner domain with the increase of the southerly and southwesterly sea breeze. From 06 to 12 UTC (0 to 6 LST), during the night and early morning hours, the mean and standard deviation of the ozone concentration in the Houston area were low because of titration from NO_x emissions and the lack of sunlight, while the southerly sea breeze gradually evolved into a strong westerly and then northwesterly land breeze (Figures 3b and 3c). In the following hours, with the increased sunlight, high $[O_3]$ with maximum over 80 ppb developed within the Houston urban plume, which extended eastward over Galveston Bay and the nearby Gulf of Mexico. Differences in the meteorological conditions result in increasing large uncertainty (spread) of $[O_3]$ which is over 15 ppb in southeast Houston and increases to over 25 ppb over Galveston Bay and over 30 ppb over Gulf of Mexico (Figure 3d). After the winds weakened and shifted from an offshore land breeze to an onshore bay/sea breeze, the ensemble mean $[O_3]$ at 21 UTC (15 LST) is ~120 ppb in the Houston area and as high as over 150 ppb over Galveston Bay (Figure 3e), which is close to the daily maximum that occurred over land an hour later. The spread of $[O_3]$ among ensemble members also increased to over

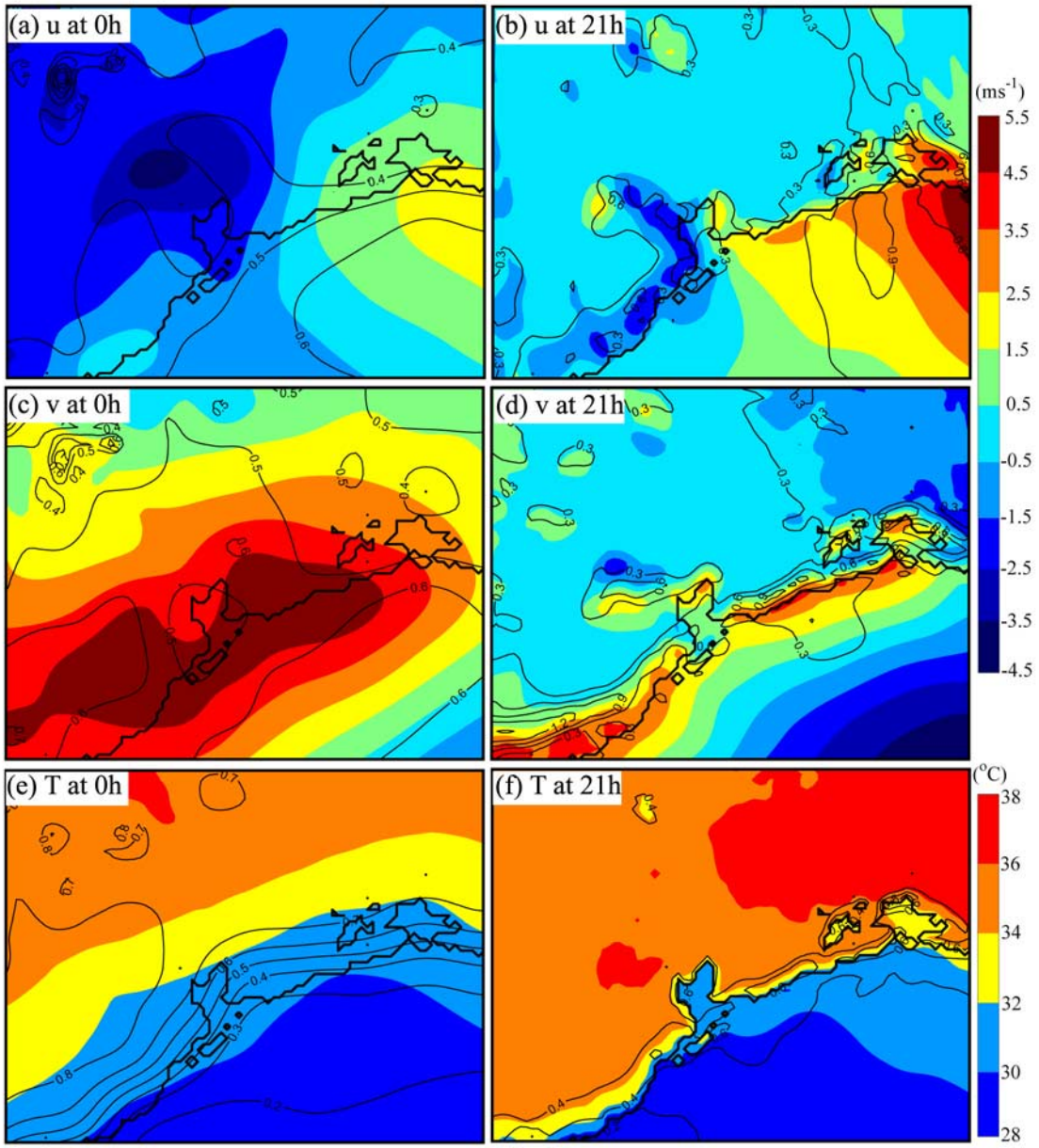

Figure 2. Ensemble mean (shown by colors) and standard deviation (shown by contours) for surface winds (m s^{-1}) (a) *u* at 0 hours, (b) *u* at 21 hours, (c) *v* at 0 hours, and (d) *v* at 21 hours, and for surface temperature *T* (°C) at (e) 0 and (f) 21 hours of the CNTL ensemble simulation. The simulation times of 0 and 21 hours correspond to 0000 UTC 30 August (18 LST 29 August) and 2100 UTC 30 August (15 LST 30 August) 2000.

20 ppb over the Houston area. Toward the end of the 24-h simulation (Figure 3f), the high ensemble mean [O_3] starts to move northward again along with the increase of southerly and southeasterly wind with the increasing sea breeze but the ensemble spread remains high in the Houston area (Figure 3f).

[16] The wind component spread was initially fairly uniform over the inner domain, while the temperature spread was relatively small over the Gulf of Mexico (Figures 2a, 2c, and 2e), reflecting the seasonal lack of variability of sea surface temperatures. The magnitude of the spread remains stable throughout the simulations, except that surface temperature spread is relatively low at night (Figure 4). However, by 2100 UTC, the ensemble spread had evolved into a pattern consistent with the meteorological situation on that day (Figures 2b, 2d, and 2f). The sea breeze, apparent in the v (north–south) component of wind, was strongest along the coast. The ensemble spread was largest just inland, associated with variability in the location of the sea breeze front. Frontal variability also produced maximum temperature spread near the coast. Because the variability is generated by an ensemble, frontal position

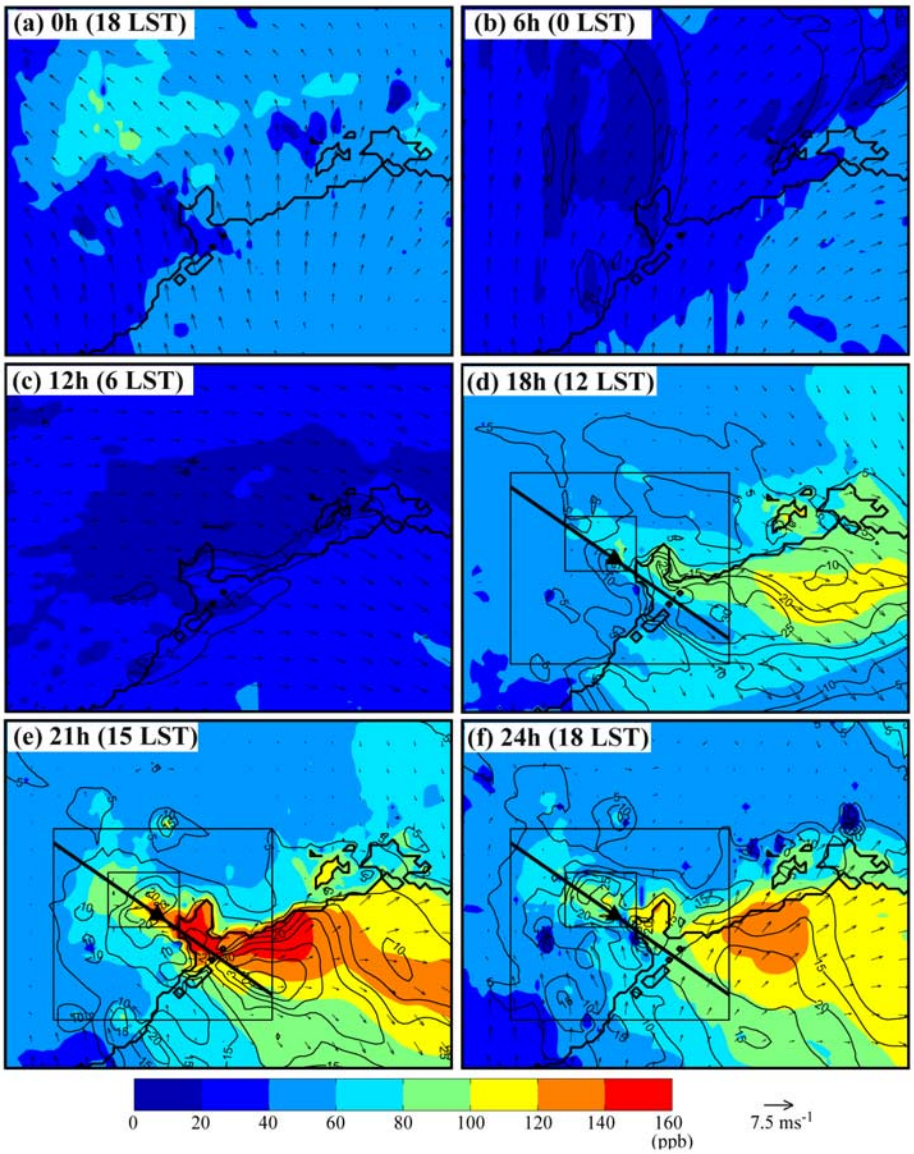

Figure 3. Ensemble mean (shown by colors) and standard deviation (shown by contours) of the surface $[O_3]$ distribution, along with ensemble mean winds valid at (a) 0 hours (b) 6 hours, (c) 12 hours, (d) 18 hours, (e) 21 hours, and (f) 24 hours of the CNTL ensemble simulations. The triangle denotes the location of the Deer Park (DRPK) station. The innermost box denotes the Houston urban core area. The larger inner box covers the same area as in Figure 1b. The lines in Figures 3d–3f denote the cross sections to be examined in Figure 8.

variations are geographically coherent and produce dynamically consistent variations in wind and temperature.

[17] Over the 24-h simulation, both the ensemble mean surface winds and $[O_3]$ compare favorably to the observations. Figure 5 shows the time evolution of the ensemble mean and spread of the ozone concentration $[O_3]$ for both the average at the 18 stations in the Houston metropolitan core area (innermost box in Figure 3e) and the Deer Park station (DRPK) that featured one of the highest observed 1-h ozone concentrations on 30 August. It is found that, for both the Houston area average and the DRPK station, the ensemble mean correctly captures the sharp buildup of $[O_3]$ from early afternoon and the peak concentration hours (>90 ppb for Houston area average and >120 ppb for DRPK from 2000 to 2300 UTC). However, the ensemble mean tends to overestimate the $[O_3]$ overnight and to underestimate the peak ozone concentration from middle to late afternoon hours.

[18] The ensemble mean winds at the surface, albeit stronger at night and smoother in transition, simulate reasonably well the diurnal cycle, especially the onset of the sea breeze (Figure 6a). Slightly above the surface, the simulated ensemble mean winds at 200 m have even better agreement with the profiler observations in terms of both the timing and amplitude (Figure 6b) but with a slight underestimation of the late morning offshore land breeze.

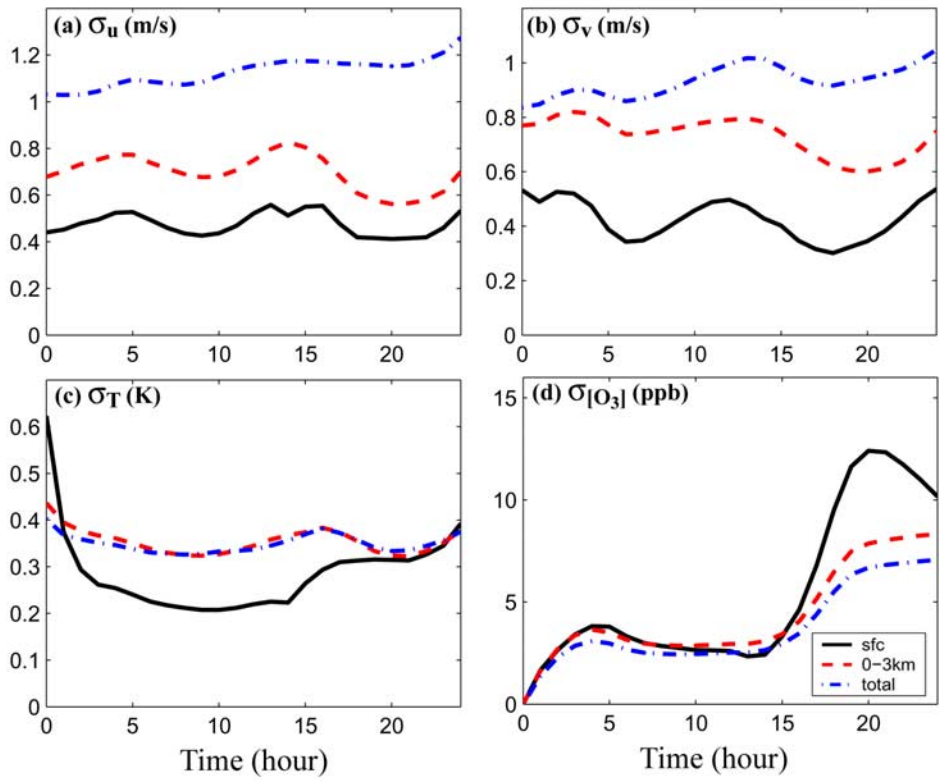

Figure 4. Time evolution of root-mean-square of the standard deviation (ensemble spread) of (a) u (m s^{-1}), (b) v (m s^{-1}), (c) T (K), and (d) [O_3] (ppb) at the surface (solid line), from 0 to 3 km (dashed line) and throughout the vertical domain (dot-dashed line) averaged over the display domains of Figures 2 and 3 of the CNTL ensemble simulation.

The overestimation of the sea breeze nighttime wind speeds at the surface and slight underestimation at 200 m by the MM5 model is likely due to a bias in the PBL parameterization [e.g., *Bao et al.*, 2005]. The ensemble mean winds and [O_3] also compare favorably to a large number of surface observations shown by *Banta et al.* [2005, Figure 4].

3.2. Uncertainties During the Peak Ozone Period

[19] Despite meteorological uncertainties (ensemble spread) in the initial conditions and in the subsequent simulations (Figures 2, 4a, 4b, and 4c) that are significantly smaller than typical observational and analysis errors (J. W. Nielsen-Gammon et al., Mesoscale model performance with assimilation of wind profiler data: Sensitivity to assimilation parameters and network configuration, submitted to *Journal of Geophysical Research*, 2006), the ensemble forecasts demonstrated great uncertainties in ozone prediction (Figures 4d and 5). For the peak ozone period in the Houston area, the maximum spread of predicted ozone concentration is greater than 5 ppb for Houston area average and over 20 ppb at the DRPK station (Figure 5). At the extremes, the maximum [O_3] at DRPK is as low as 90 ppb in one ensemble member but is as high as 160 ppb in another member (Figure 5b), which spanning by a wide margin the US EPA 1-h ozone standard of 124 ppb. The Houston area averaged observed [O_3] is mostly within the spread of the ensemble simulations during its peak hours. However, the stationwise 1-h observation at DRPK is slightly larger than the maximum value predicted by any ensemble member, indicating that deficiencies still exist in the ensemble simulation. Such difficulties can arise from initial condition errors and model uncertainties in both the meteorological and photochemical models as well as uncertainties in the emission inventory.

[20] To illustrate the disparity between different ensemble members, the surface [O_3] along with surface winds and potential temperature from two ensemble members are displayed: member 1 (EN1) has one of the lowest [O_3] at DRPK (Figures 7a, 7c, and 7e) and member 6 (EN6) has one of the highest at DRPK (Figures 7b, 7d, and 7f). Differences in the surface winds between these two extreme members are apparent and are closely related to the dramatic difference in [O_3] over DRPK and Houston in the afternoon. In particular, the large-scale winds (along with the late morning offshore land breeze) have a much stronger northerly component in EN6 than in EN1 at 1500 UTC (9 LST; Figures 7a–7b), which appears to result in more pollutants over Galveston Bay than over the land area northeast of the Bay area in EN6 at 1800 UTC (noon LST; Figures 7c–7d). EN1 still had most of the Houston plume over land at that time. In the meantime, lighter overall wind speeds in EN6 contribute to higher [O_3] within the urban plume. Finally, the reversal of wind directions over Galveston Bay also occurs earlier in EN6 than EN1. An earlier reversal of the wind direction (in the form of sea/bay breeze) will lead to transport of more polluted air back to Houston while the environment is still photochemically active. The surface

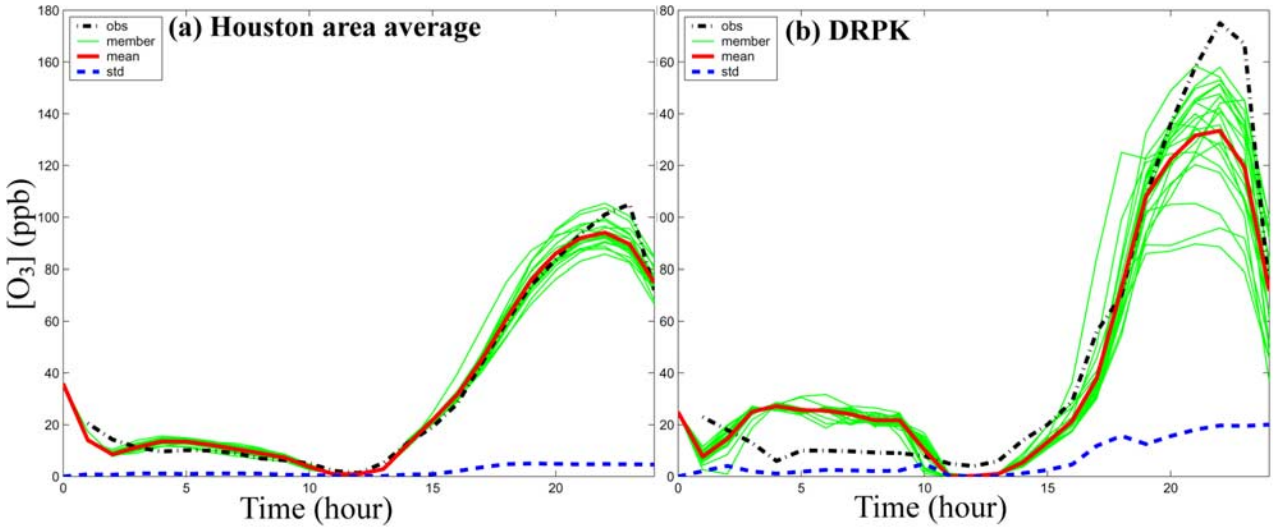

Figure 5. Time evolution of the surface $[O_3]$ (ppb) from each ensemble member (thin green lines), ensemble mean (bold orange line), standard deviation (dashed line) of the CNTL ensemble simulation and real-time observations (dot-dashed line) for (a) values averaged over the Houston urban core area (innermost box of Figures 1b, 3d, 3e, and 3f) and (b) the DRPK station.

$[O_3]$ at DRPK and over the entire Houston urban is thus much higher in EN6 than in EN1 (Figures 7e–7f).

[21] Much larger uncertainty is found in point forecasts of ozone (e.g., at DRPK) than in an area average of ozone over the Houston urban core area (Figure 5). Consideration of individual ensemble members EN1 and EN6 (Figure 7) shows that simulated differences in the position of the localized $[O_3]$ maximum inside the averaging domain may have contributed significantly to the discrepancy between stationwise and area-averaged ensemble spreads.

3.3. Verification of the Multistage Schematics of *Banta et al.* [2005]

[22] Using observations from the surface network, wind profilers, and an airborne ozone lidar made during 30 August as part of the Texas 2000 Air Quality Study (TexAQS2000), *Banta et al.* [2005] presented a multistage schematic model showing the effects of the daytime sea breeze on the high ozone concentrations of 30 August: (1) During the morning and early afternoon period, the large-scale offshore northwesterly flow along with the weakening land breeze carries the pollution from the Houston urban and Ship-Channel areas over Galveston Bay, resulting in low ozone concentrations over the land; (2) from middle to late afternoon hours, the onset of onshore sea/bay breeze brings the previously offshore transported urban pollutants into a convergence zone along the coastline, which along with the buildup of emissions due to nearly stagnant flow, results in the highest $[O_3]$ observed in eastern Houston [*Banta et al.*, 2005, Figure 8]; and (3) in the evening hours, the

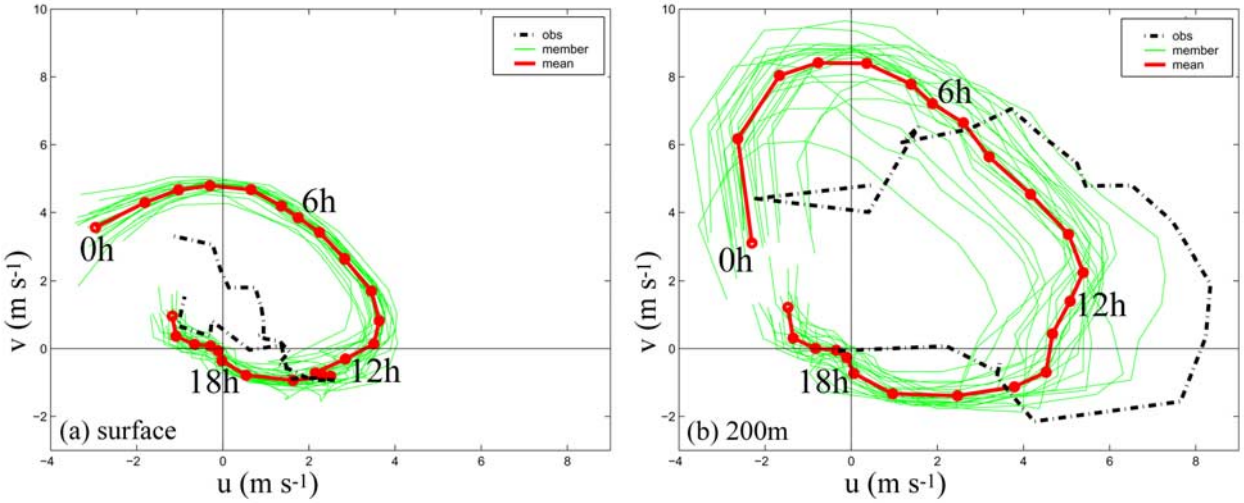

Figure 6. The CNTL ensemble simulated and observed wind hodographs averaged over the Houston urban core area at (a) surface and (b) 200 m. The 200-m wind observations are the average of two profilers at Wharton and Houston Southwest (both locations denoted in Figure 1b).

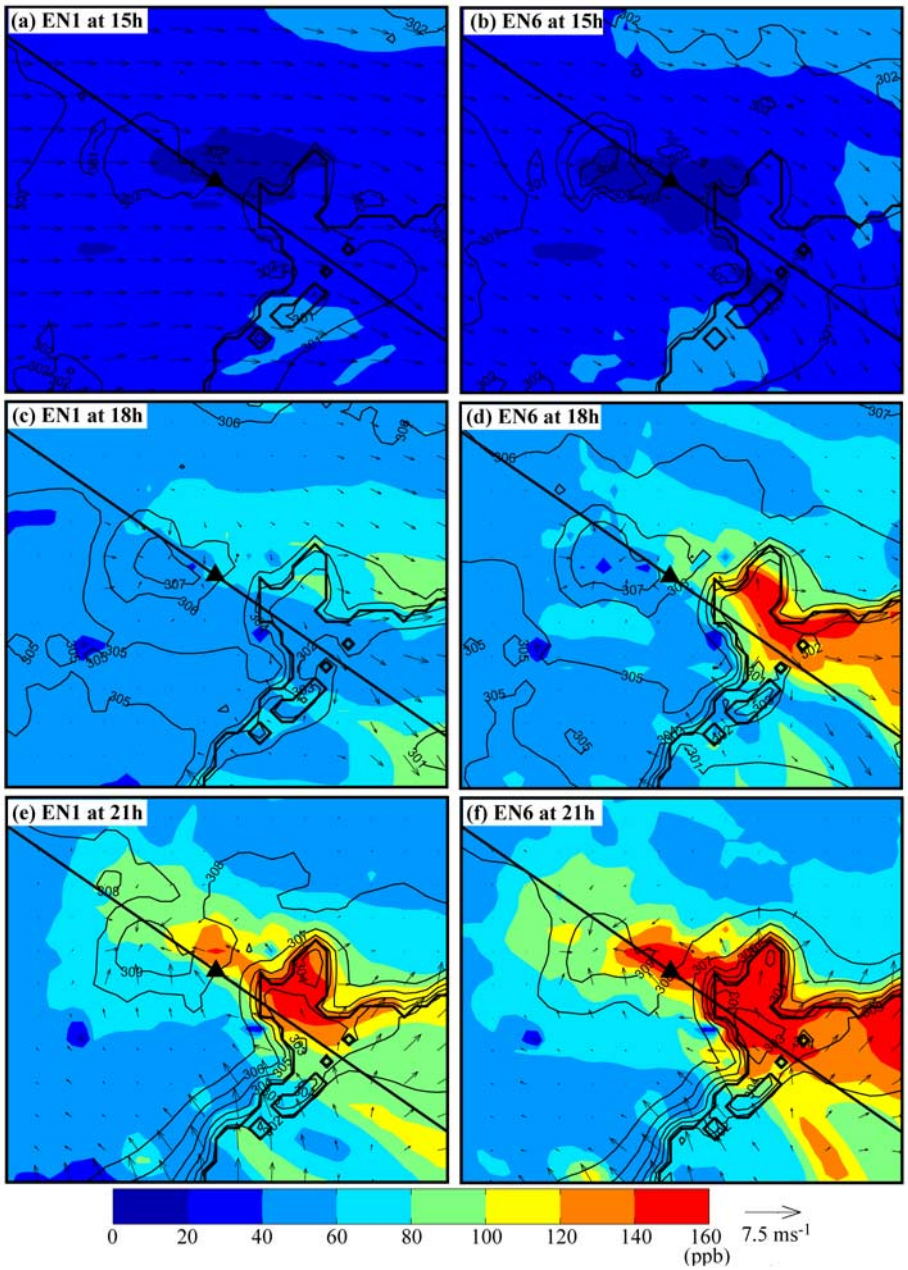

Figure 7. Ozone concentration (shown by colors) and potential temperature (shown by contours) of two ensemble members (EN1 and EN6) in a smaller domain (inner box denoted in Figures 3d–3f) valid at (a–b) 15 hours, (c–d) 18 hours, and (e–f) 21 hours.

increasing onshore sea breeze transports the pollutants farther inland to rural areas resulting in declining ozone concentrations in the urban Houston area.

[23] The mean simulations by the meteorological and photochemical ensembles agree well with and further solidify the multistage schematics of *Banta et al.* [2005]. The ensemble mean potential temperature, vertical velocity, and wind circulations in a vertical section (location depicted in Figure 3) nearly perpendicular to the coast and through DRPK are shown in Figures 8a, 8c, and 8e. The ensemble mean and spread of [O_3] and ensemble mean winds and the maximum [O_3] along the same vertical section are displayed in Figures 8b, 8d, and 8f.

[24] At 1800 UTC (12 LST, noontime), as in observations of *Banta et al.* [2005], a strong land breeze is present offshore and a deep marine boundary layer extends from Galveston Bay to the Gulf of Mexico with PBL heights increasing with distance offshore (Figure 8a). In the meantime, daytime heating leads to the development of a 1.5–2.5-km deep daytime convective boundary layer over land. The PBL is deepest over the center of Houston, where the simulated urban heat island effect has resulted in two centers of ascending motions and convergence (which correspond to the two urban land use centers in Figure 1b). The surface horizontal winds from the coast inland are mostly stagnant at this time in both model and observations.

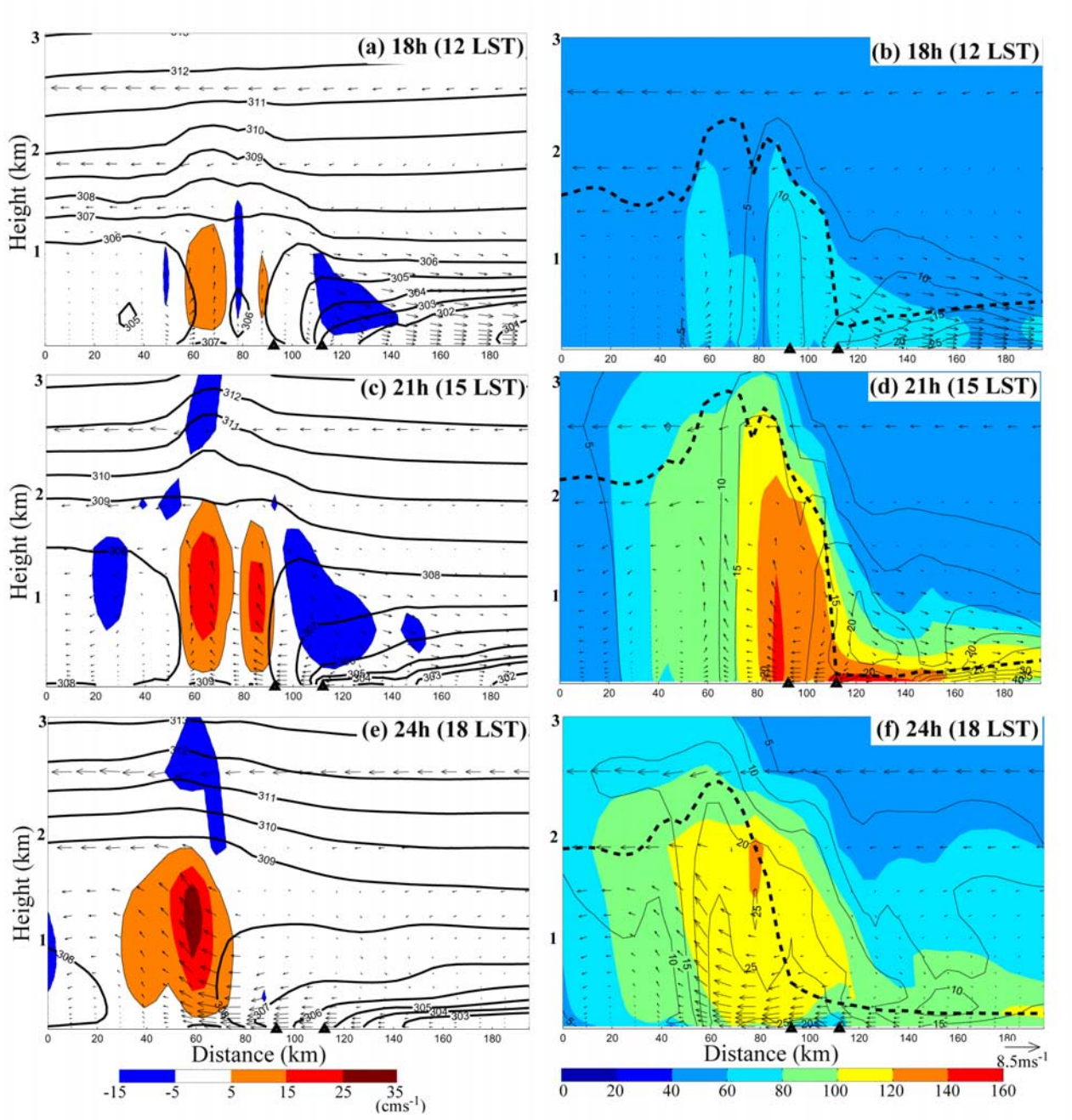

Figure 8. (a–b) Vertical section of (Figure 8a) vertical velocity (shown by colors), potential temperature (contoured, K), and wind vectors along the cross section (scaled proportionally) and (Figure 8b) ensemble mean and standard deviations (every 5 ppb) of [O_3] along with PBL top (dashed line) and wind vectors valid at 18 h; (c–d) As in Figures 8a–8b but at 21 h; (e–f) As in Figures 8a–8b but at 24 hours of the CNTL ensemble simulation. The location of the vertical section is denoted as the dark black line in Figures 3d–3f. The left triangle denotes the location of DRPK, and the right triangle denotes the coast line.

Although difficult to verify, a surface wind reversal (and thus the onset of the bay breeze) begins in a narrow region right along the coast of Galveston Bay (Figure 8a).

[25] Throughout the later morning to early afternoon hours, the offshore land breeze continuously transports the pollutants from the Houston area to over the water, resulting in elevated [O_3] (over 80 ppb) throughout the deep marine boundary layer over Galveston Bay and the Gulf waters (Figure 8b). In the meantime, the decreasing wind speeds and high temperatures over land lead to ozone production and moderate concentrations (>80 ppb) over the urban Houston area. The spread of [O_3] is rather uniform through

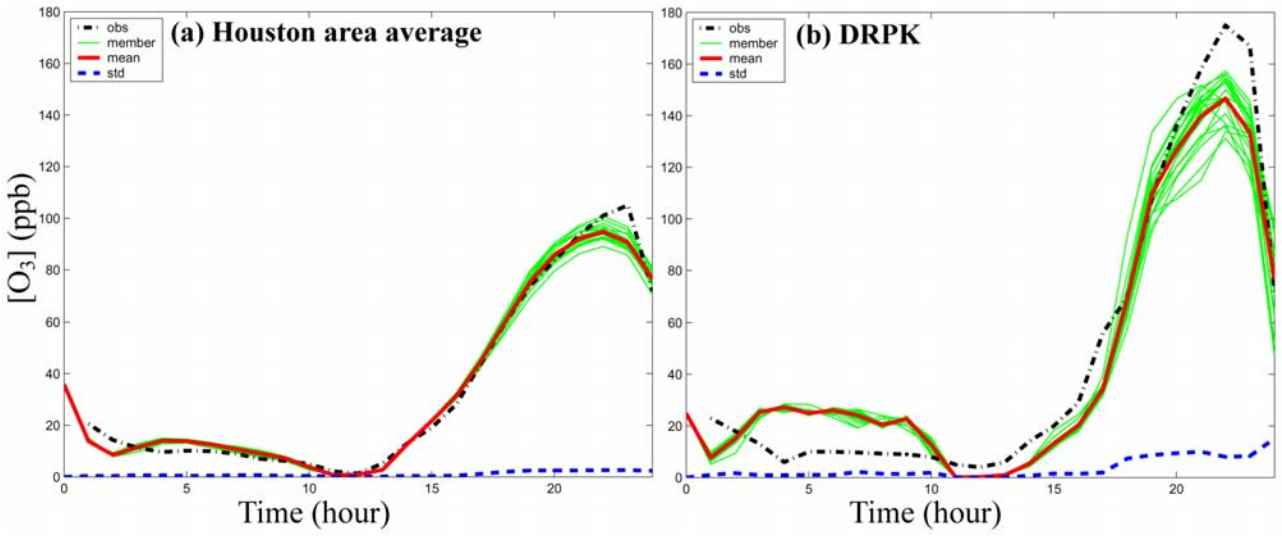

Figure 9. As in Figure 5 but for experiment "half-run".

the boundary layer over land but increases with distance offshore, from around 15 ppb near coast to over 25 ppb over Gulf of Mexico (Figure 8b). The increasing spread is caused partly by increasing ozone levels as the urban plume ages and increasing uncertainty in plume location.

[26] From early to mid-afternoon, the marine boundary layer becomes shallower and more stable as increasingly warm air is advected offshore and the onset of the sea breeze produces subsidence over the nearshore waters. At 2100 UTC (15 LST), the onshore sea/bay breeze has intruded inland, passing DRPK in the ensemble mean. The distinctive "ozone wall" at the coastline, with maximum ozone concentration of over 140 ppb an hour later at DRPK, is somewhat weak but otherwise consistent with the observations reported by *Banta et al.* [2005]. The simulated ozone wall is produced by a combination of factors: (1) Vertical wind shear during morning transport produces a shallow layer of ozone precursors over water. (2) The sea breeze carries the earlier offshore transported pollutants back to Houston, where they enter a progressively deeper boundary layer and mix vertically. (3) The air into which the sea breeze penetrates has been stagnant for several hours over the industrial Ship Channel area, where high concentrations of ozone and ozone precursors have developed from local emissions. Surface temperatures in excess of 35°C doubtless contributed to the unusually high ozone levels. The model produces a double peak in ozone: a deep maximum near 90 km and a shallow maximum near 120 km. This structure is consistent with observations at La Porte, between DRPK and the coastline, where two separate peaks of ozone over 160 ppb were observed before and after the arrival of the sea breeze front [*Banta et al.*, 2005].

[27] The standard deviation of [O_3] also increases significantly during this period, reaching 20 ppb just northwest of DRPK near the surface but over 15 ppb over most the deep boundary layer over Houston. The spread becomes even stronger over the eroding marine boundary layer, exceeding 20 ppb over Galveston Bay and 40 ppb over the Gulf of Mexico. There is also a separate spread maximum (>20 ppb) above the marine boundary layer just east of the ozone wall along the coast (Figure 8d).

[28] In the late afternoon, the bay/gulf breeze prevails along the vertical section and the sea breeze has transported the high [O_3] farther inland (Figures 8e and 8f). In the meantime, the sea breeze also brings cleaner air from the Bay and Gulf as the earlier urban plume has been advected northward out of the vertical section. After this time, along with the decreasing air temperature, [O_3] decreases significantly at the surface over land (Figure 8f). However, this is accompanied by even larger ensemble spread over this area at this time, likely due to uncertainties in the sea breeze circulation and larger-scale meteorological conditions.

4. Sensitivity Ensemble Experiments

[29] Experiments "half-run" ("double-run") are performed exactly the same as CNTL for both the meteorological and photochemical ensembles except that the initial ensemble perturbations (i.e., the meteorological initial uncertainty) are linearly reduced by half (doubled). These two experiments aim to examine the influence of the meteorological error amplitude in ozone pollution simulation uncertainties. From the evolution of the ensemble mean and standard deviation of [O_3] for the Houston area average and the DRPK station (Figures 9 and 10), it is found that the ensemble means from both experiments are qualitatively similar to that of the CNTL experiment when averaged over the Houston area. At DRPK, the ensemble mean peak ozone progressively decreases as the ensemble perturbations are increased. In other words, large departures from the CNTL meteorology are more likely than small departures to produce lower ozone. Apparently, the CNTL meteorological conditions are near optimal for high ozone at this station, since perturbations from CNTL are biased toward lower ozone.

[30] The spread is much smaller (larger) in the half-run (double-run) because of reduced (increased) uncertainties in the meteorological initial conditions. Nevertheless, the

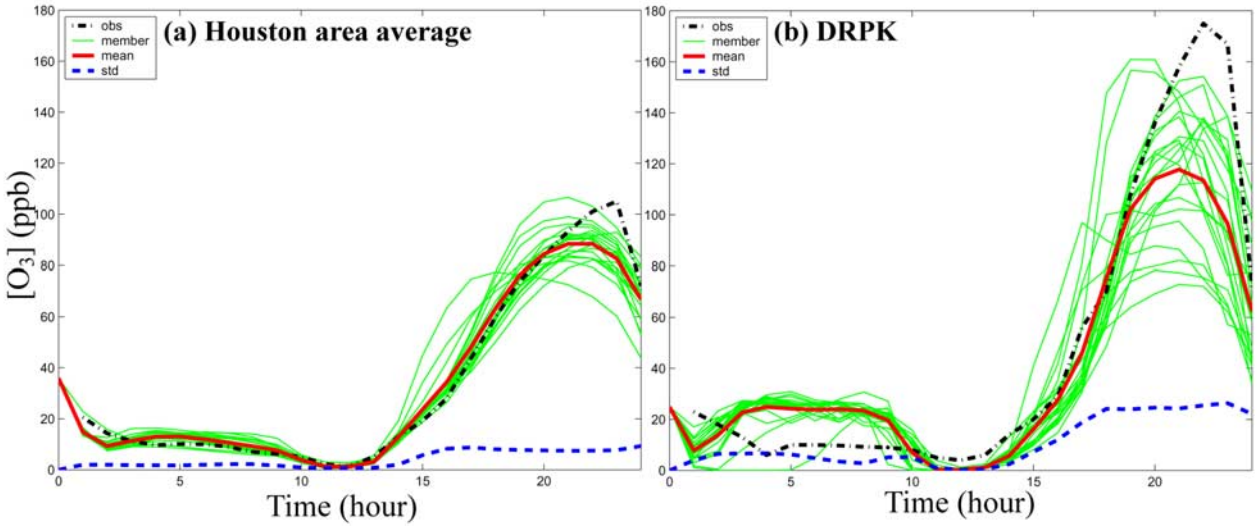

Figure 10. As in Figure 5 but for experiment "double-run".

response in $[O_3]$ simulation uncertainty is not strictly linear since the simulated ensemble spread in half-run (double-run) is generally larger (smaller) than half (double) of that in CNTL.

[31] The evolution of the root-mean-square of the ensemble spread of u, v, T and $[O_3]$ at the surface, from 0 to 3 km and throughout the vertical domain from the half-run and double-run are respectively displayed in Figures 11 and 12. For the half-run (double-run), by reducing (increasing) the

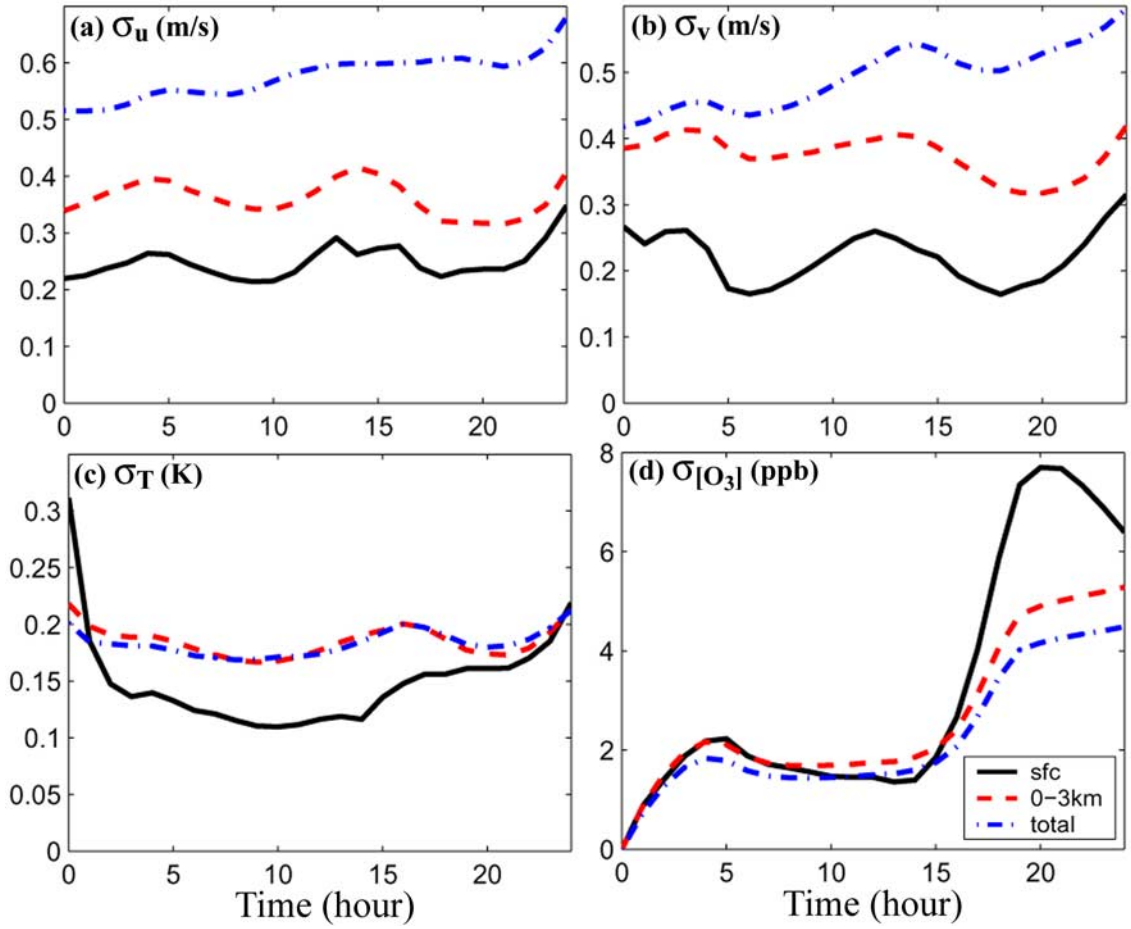

Figure 11. As in Figure 4 but for experiment "half-run".

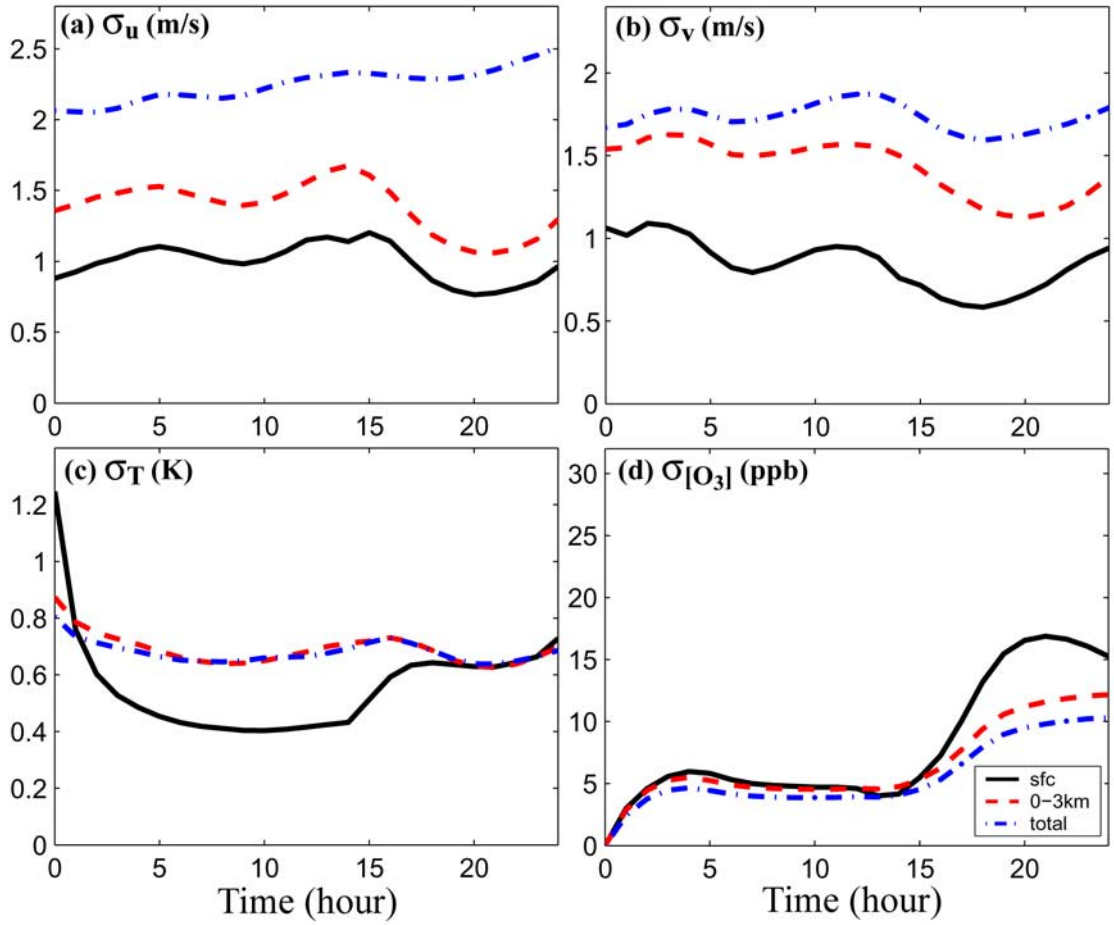

Figure 12. As in Figure 4 but for experiment "double-run".

initial ensemble perturbation amplitude to half (twice) of the initial ensemble spread in CNTL, the ensemble spread of u, v, and T in subsequent hours are also nearly half (twice) of those in CNTL. The ensemble spread of $[O_3]$ in half-run is also nearly reduced by half (and thus almost linearly) but interestingly it is increased by less than twice in the double-run, indicating nonlinear correlations of $[O_3]$ with the meteorological conditions when the uncertainties are large.

[32] We also examined the PBL height uncertainties caused by the initial meteorological errors. PBL height uncertainties increase nearly linearly with the linear increase of amplitude of the initial meteorological errors in these two sensitivity ensemble experiments (not shown), but overall PBL height variability over land is too small to contribute to the ozone variability.

[33] These sensitivity experiments strongly suggest that reducing the uncertainties in the meteorological conditions, through either better data assimilation or denser or more accurate observations, can significantly reduce the uncertainty in the ozone simulation and prediction.

5. Summary and Discussion

[34] We examined the uncertainties in the ozone prediction due to uncertainties in the meteorological simulations through performing 24-h meteorological and photochemical ensemble simulations of Houston area ozone at 4-km resolution. The 21-member ensembles are initiated at 00Z 30 August 2000 using climatological error randomly selected from the Eta model GCIP analysis data sets from 1 June to 15 September 2000. The 24-h ensemble mean simulations of meteorological conditions and ozone concentrations agreed fairly well with the observations.

[35] We found dramatic uncertainties in the ozone prediction in Houston and surrounding areas due to meteorological uncertainties. The sensitivity ensemble experiments indicate that the ensemble means from both experiments are qualitatively similar to that of the CNTL experiment while the ensemble spread is much smaller (larger) in "half-run" ("double-run") because of reduced (increased) uncertainties in the meteorological conditions, though the response is not strictly linear.

[36] The current ensemble approach differs from the past Monte Carlo approaches [e.g., *Hanna et al.*, 2001; *Beekmann and Derognat*, 2003] in that (1) initial perturbations sampled from scaled warm season climatological uncertainties are realistic in nature which include initial condition errors at both the large scale and mesoscale; and (2) initial perturbations in different meteorological variables are dynamically consistent and mostly balanced. The nonlinear response of the ozone concentration uncertainty as

demonstrated from experiments "half-run" and "double-run", albeit weak, may also not be revealed with the adjoint sensitivity approach [e.g., *Menut*, 2003].

[37] The high uncertainties in the ozone simulation for the Houston area from the high-resolution photochemical model clearly demonstrate the importance of accurate representation of meteorological conditions in this event. However, even with plentiful observations, analysis inaccuracies are unavoidable, so a single-minded pursuit of improved initial conditions is inadvisable. Instead, ensemble simulations should be utilized to span the range of possible outcomes consistent with the meteorological conditions on a given day, and that uncertainty should be incorporated into the regulatory analysis. If deterministic simulations are required for regulatory purposes, perhaps the best-performing ensemble member can be selected for further analysis, pending confirmation that improved ozone performance is accompanied by improved meteorological performance. Cases may be selected on the basis of low meteorology-driven uncertainty, reducing the likelihood that a meteorological error is compensating for an emissions or chemistry error.

[38] As with simulations, deterministic photochemical forecasts are similarly unlikely to be successful. Initial condition uncertainty is only one of several known sources of significant photochemical model error [*Hanna et al.*, 2001]. The fact that no ensemble members produced ozone as high as what was observed at Deer Park is clear evidence that other errors in the model or emissions are adversely affecting the simulations. An ensemble forecasting system, incorporating as many sources of error as possible, can provide guidance on both the most likely ozone evolution but also the range of possibilities.

[39] **Acknowledgments.** This research was funded by GTRI/HARC grant project H24-2003, NSF grant ATM-0205599, and ONR grant N000140410471.

References

Aksoy, A., F. Zhang, J. W. Nielsen-Gammon, and C. C. Epifanio (2005), Data assimilation with the ensemble Kalman filter for thermally forced circulations, *J. Geophys. Res.*, *110*, D16105, doi:10.1029/2004JD005718.

Aksoy, A., F. Zhang, and J. W. Nielsen-Gammon (2006), Ensemble-based simultaneous state and parameter estimation in a two-dimensional sea breeze model, *Mon. Weather Rev.*, *134*, 2951–2970.

Banta, R. M., et al. (2005), A bad air day in Houston, *Bull. Am. Meteorol. Soc.*, *86*, 657–669.

Bao, J.-W., S. A. Michelson, S. A. McKeen, and G. A. Grell (2005), Meteorological evaluation of a weather-chemistry forecasting model using observations from the TEXAS AQS 2000 field experiment, *J. Geophys. Res.*, *110*, D21105, doi:10.1029/2004JD005024.

Beekmann, M., and C. Derognat (2003), Monte Carlo uncertainty analysis of a regional-scale chemistry model constrained by measurements from the Atmospheric Pollution Over the Paris Area (ESQUIF) campaign, *J. Geophys. Res.*, *108*(D17), 8559, doi:10.1029/2003JD003391.

Bergin, M. S., G. S. Noblet, K. Petrini, J. R. Dhieux, J. B. Milford, and R. A. Harley (1999), Formal uncertainty analysis of a Lagrangian photochemical air pollution model, *Environ. Sci. Technol.*, *33*, 1116–1126.

Byun, D. W., and J. K. S. Ching (Ed.) (1999), Science algorithms of the EPA models-3 Community Multi-scale Air Quality (CMAQ) Modeling System, *Rep. EPA/600/R-99/030*, Natl. Exposure Res. Lab., Research Triangle Park, N. C.

Dabberdt, W. F., and E. Miller (2000), Uncertainty, ensembles and air quality dispersion modeling: Applications and challenges, *Atmos. Environ.*, *34*, 4667–4673.

Dabberdt, W. F., et al. (2004), Meteorological research needs for improved air quality forecasting: Report of the 11th Prospectus Development Team of the U.S. Weather Research Program, *Bull. Am. Meteorol. Soc.*, *85*, 563–586.

Darby, L. S. (2005), Cluster analysis of surface winds in Houston, Texas, and the impact of wind patterns on ozone, *J. Appl. Meteorol.*, *44*, 1788–1806.

Delle Monache, L., and R. Stull (2003), An ensemble air quality forecast over western Europe during an ozone forecast, *Atmos. Environ.*, *37*, 3469–3474.

Delle Monache, L., X. Deng, Y. Zhou, and R. Stull (2006a), Ozone ensemble forecasts: 1. A new ensemble design, *J. Geophys. Res.*, *111*, D05307, doi:10.1029/2005JD006310.

Delle Monache, L., T. Nipen, X. Deng, Y. Zhou, and R. Stull (2006b), Ozone ensemble forecasts: 2. A Kalman-filter predictor bias correction, *J. Geophys. Res.*, *111*, D05308, doi:10.1029/2005JD006311.

Dudhia, J. (1993), A nonhydrostatic version of the Penn State-NCAR Mesoscale Model: Validation tests and simulation of an Atlantic cyclone and cold front, *Mon. Weather Rev.*, *121*, 1493–1513.

Environmental Protection Agency (EPA) (2003), Models-3 Community Multiscale Air Quality (CMAQ) model, version 4.3, report, Research Triangle Park, N.C. (Available at http://www.cmascenter.org/modelclear.shtml)

Estoque, M. (1962), The sea breeze as a function of the prevailing situation, *J. Atmos. Sci.*, *19*, 244–250.

Fine, J., L. Vuilleumier, S. Reynolds, P. Roth, and N. Brown (2003), Evaluating uncertainties in regional photochemical air quality modeling, *Annu. Rev. Environ. Resour.*, *28*, 59–106.

Galmarini, S., et al. (2004a), Can the confidence in long range atmospheric transport models be increased? The Pan-European experience of ENSEMBLE, *Radiat. Prot. Dosimetry*, *109*, 19–24.

Galmarini, S., et al. (2004b), Ensemble dispersion forecasting–Part I: Concept, approach and indicators, *Atmos. Environ.*, *38*, 4607–4617.

Galmarini, S., et al. (2004c), Ensemble dispersion forecasting–Part II: Application and evaluations, *Atmos. Environ.*, *38*, 4619–4632.

Grell, G. A. (1993), Prognostic evaluation of assumptions used by cumulus parameterizations, *Mon. Weather Rev.*, *121*, 764–787.

Hanna, S. R., Z. G. Lu, H. C. Frey, N. Wheeler, J. Vukovich, S. Arunachalam, M. Fernau, and D. A. Hansen (2001), Uncertainties in predicted ozone concentrations due to input uncertainties for the UAM-V photochemical grid model applied to the July 1995 OTAG domain, *Atmos. Environ.*, *35*, 891–903.

Hogrefe, C., et al. (2001), Evaluating the performance of regional-scale photochemical modeling systems: Part I–Meteorological predictions, *Atmos. Environ.*, *35*, 4159–4174.

Hong, S.-Y., and H.-L. Pan (1996), Nonlocal boundary layer vertical diffusion in a medium-range forecast model, *Mon. Weather Rev.*, *124*, 2322–2339.

Irwin, J. S., S. T. Rao, W. B. Petersen, and D. B. Turner (1987), Relating error-bounds for maximum concentration estimates to diffusion meteorology uncertainty, *Atmos. Environ.*, *21*, 1927–1937.

Kalnay, E. (2003), *Atmospheric Modeling, Data Assimilation and Predictability*, 341 pp, Cambridge Univ. Press, New York.

Mallet, V., and B. Sportisse (2006), Uncertainty in a chemistry-transport model due to physical parameterizations and numerical approximations: An ensemble approach applied to ozone modeling, *J. Geophys. Res.*, *111*, D01302, doi:10.1029/2005JD006149.

McKeen, S. A., et al. (2005), Assessment of an ensemble of seven real-time ozone forecasts over eastern North America during the summer of 2004, *J. Geophys. Res.*, *110*, D21307, doi:10.1029/2005JD005858.

Menut, L. (2003), Adjoint modeling for atmospheric pollution process sensitivity at regional scale, *J. Geophys. Res.*, *108*(D17), 8562, doi:10.1029/2002JD002549.

Pagowski, M., et al. (2005), A simple method to improve ensemble-based ozone forecasts, *Geophys. Res. Lett.*, *32*, L07814, doi:10.1029/2004GL022305.

Rotunno, R. (1983), On the linear theory of the land and sea breeze, *J. Atmos. Sci.*, *40*, 1999–2009.

Ryerson, T. B., et al. (2003), Effect of petrochemical industrial emissions of reactive alkenes and NO_x on tropospheric ozone formation in Houston, Texas, *J. Geophys. Res.*, *108*(D8), 4249, doi:10.1029/2002JD003070.

Simpson, J. E. (1994), *Sea Breeze and Local Wind*, 234 pp., Cambridge Univ. Press, New York.

Straume, A. G. (2001), A more extensive investigation of the use of ensemble forecasts for dispersion model evaluation, *J. Appl. Meteorol.*, *40*, 425–445.

Stuart, A. L., S. Jain, and S. B. Libicki (1996), The use of long-term meteorological information to predict impact probabilities resulting from toxic chemical releases, in *Proceedings of the International Topical Meeting of Probabilistic Safety Assessment*, Am. Nuclear Soc., La Grange Park, Ill.

Warner, T. T., et al. (2002), Ensemble simulations with coupled atmospheric dynamic and dispersion models: Illustrating uncertainties in dosage simulations, *J. Appl. Meteorol.*, *41*, 488–504.

Wert, B. P., et al. (2003), Signatures of terminal alkene oxidation in airborne formaldehyde measurements during TexAQS 2000, *J. Geophys. Res.*, *108*(D3), 4104, doi:10.1029/2002JD002502.

Yegnan, A., D. G. Williamson, and A. J. Graettinger (2002), Uncertainty analysis in air dispersion modeling, *Environ. Modell. Software*, *17*, 639–649.

Zhang, R., W. Lei, X. Tie, and P. Hess (2004), Industrial emissions cause extreme diurnal urban ozone variability, *Proc. Natl. Acad. Sci. U. S. A.*, *101*, 6346–6350.

A. Aksoy, Mesoscale and Microscale Meterorology Division, National Center for Atmospheric Research, P.O. Box 3000, Boulder, CO 80307-3000, USA.

N. Bei, G. Li, J. W. Nielsen-Gammon, F. Zhang, and R. Zhang, Department of Atmospheric Sciences, Texas A&M University, College Station, TX 77843-3150, USA. (fzhang@tamu.edu)

A. Stuart, Department of Environmental and Occupational Health, University of South Florida, 13201 Bruce B. Downs Boulevard, MDC-56, Tampa, FL 33612, USA.